CHEMISTRY
A EUROPEAN JOURNAL

DOI: 10.1002/chem.200700178

# Molecular Optical Switches: Synthesis, Structure, and Photoluminescence of Spirosila Compounds

**Duanchao Yan, Javad Mohsseni-Ala, Norbert Auner,* Michael Bolte, and Jan W. Bats[a]**

**Abstract:** Starting from a silicon dichloro substituted silole and a silacyclobutene, a series of new organosilicon-based spiro compounds was synthesized by using standard organometallic reaction procedures. The spiro compounds that combine two organic photoactive subunits at one silicon center were fully characterized by the usual analytical and spectroscopic methods, which include molecular structure determination by single-crystal X-ray analysis. Photoluminescence spectra of the compounds were recorded in the solid state and also as dilute solutions in THF. Interpretation of the spectra revealed that photoluminescence in this series of compounds originated from the stilbene or its vinylogue subunits. Different linkages of these groups to the silicon atoms (cyclic or open structures, four- or five-membered cycles) strongly affected both the excitation and the emission spectra, which show different emission maxima depending on the state of the sample (solid state or in solution) and the wavelength of light used for excitation. Thus, owing to their optoelectronic properties these compounds might be useful tools for the design of sensitive sensor materials and of optical switches.

**Keywords:** fluorescence · optical switches · silanes · silicon · spiro compounds

## Introduction

Organic electroluminescent devices based on organic or organometallic frameworks, which are generally composed of thin multilayers of hole-transporting, emissive, and electron-transporting materials that are sandwiched between two electrodes,[1,2] have received much attention because of their possible application as new display materials.[3] Some unsaturated ring compounds that contain silicon, such as siloles[4a–c] and silacyclobutenes,[4d] exhibit strong photoluminescence emission in the solid state as well as a strong aggregation-induced photoluminescence, which is a favored characteristic for materials applications.

Spiro functionalized compounds that contain a silicon center surrounded by four carbon atoms are of general interest because they may serve as starting materials for the preparation of macromolecules and polymers with interesting physical properties.[5] Both the polymers and the monomeric building units have useful nonlinear optical properties.[6] Owing to their transparency, they may serve as tools for the formation of organic electroluminescent devices.[7]

Investigations into silaspirene molecules with tailor-made optoelectronic physical properties that result from the unsaturated carbon–carbon π bonds within the spiro ring systems[7a,8] are rather limited. Most of the spiro compounds reported to date contain five-membered silacycloalkene ring subunits in their molecular backbone.[8,9] To the best of our knowledge, no paper has yet been published that deals with pure silaspiro[3,3]hept-1,5-dienes, which are small-ring silaspirenes that might be important compounds for both theoretical studies and experimental applications. There is one recent publication by Pellny et al. that discusses 2-phenyl-4-benzylidene-1-silacyclobut-2-ene (PBSE) complexes of zirconocene and titanocene, in which the organometallic fragments bridge the 1,5-dibenzylidene-3,7-diphenyl-4-silaspiro-[3,3]hept-1,5-diene unit twice.[10] In this paper we report the syntheses and molecular structures of several silaspirenes, silaspiro[3,4]octa-1,5,7-triene (**6**), which is a combination of a PBSE subunit with a 2,3,4,5-tetraphenyl-1-silacyclopenta-2,4-diene (silole) ring; silaspiro[3,3]hept-1,5-diene (**7**), which combines a PBSE subunit with a 2,3-diphenyl-3-neopentyl-1-silacyclobut-2-ene (DNSE) subunit; spiro compound **10**,[9] which is a combination of a silole ring and a silafluorene; and spirosilole **2**, which consists of two silole rings. Subsequently, their UV-visible and fluorescence spectra were

[a] Dr. D. Yan, Dr. J. Mohsseni-Ala, Prof. Dr. N. Auner, Dr. M. Bolte, Dr. J. W. Bats
Institut für Anorganische Chemie der
Johann Wolfgang Goethe-Universität
Max-von-Laue-Strasse 7, 60438 Frankfurt (Germany)
Fax: (+49) 69-798-29188
E-mail: Auner@chemie.uni-frankfurt.de

measured and are discussed in comparison with the data for the monocyclic building blocks **4** (silole), **5** (DNSE), and silafluorene **13** and **14** (PBSE), to investigate the influence of the silicon spiro bridges on the optoelectronic properties of the silaspirenes.

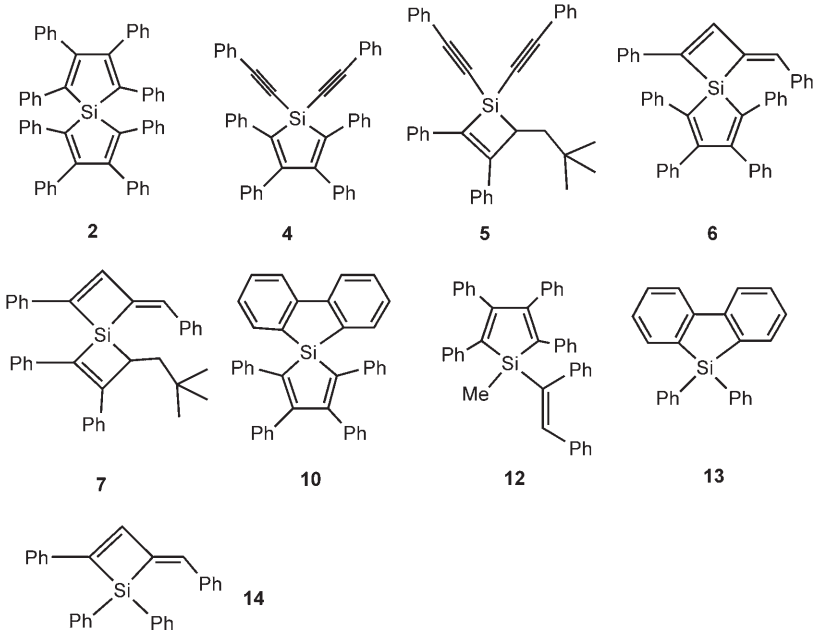


## Results and Discussion

Following published procedures, 1,1-dichlorosilacyclopentadiene (**1**)[11] and octaphenyl-1,1′-spirobisilole (**2**)[12] were synthesized by treatment of 1,4-dilithiotetraphenylbutadiene with tetrachlorosilane (Scheme 1). 1,1-Dichlorosilacyclobutene (**3**)[13] was prepared by addition of *tert*-butyllithium to a solution of tolane and vinyltrichlorosilane (Scheme 1). Reaction of 1,1-dichlorosilanes **1** or **3** with PhC≡CMgBr (2 equiv) at room temperature in THF gave crystalline bis(alkynyl)-substituted silacyclic compounds **4**[4b] and **5** in yields of 73 and 86%, respectively.[14] Subsequent treatment of solutions of compounds **4** or **5** in THF with (cyclopentadienyl)ethyl zirconocene (Takahashi's reagent, 1 equiv)[15a] at −35 °C for 14 h, followed by hydrolysis of the reaction mixtures with 3 N aqueous HCl, resulted in the formation of silaspirenes **6** and **7** as crystalline solids in yields of 26 and 69%, respectively. The two silaspirenes were purified and isolated by column chromatography. It is proposed that a mixture of **4** or **5** and [Zr($C_2H_4$)Cp] leads to the formation of zirconocene complexes **8** and **9** as intermediates in a reaction pathway that is analogous to that observed for reactions of Takahashi's reagent with bis(alkynyl)silanes, which have been extensively investigated.[15b] Upon hydrolysis of complexes **8** and **9**, **6** and **7** are formed through intramolecular coupling reactions of alkynyl groups (Scheme 2). Spirosilole **10** was obtained from a one-pot reaction of dichlorosilole **1** with 2,2′-dilithiobiphenyl, which was synthesized in situ by treating 2,2′-dibromobiphenyl with *n*BuLi (2 equiv) in diethyl ether (Scheme 3). 1,1-Dichlorosilane **11** was prepared by hydrosilylation of tolane with methyldichlorosilane in the presence of [$PtCl_6H_2$] as a catalyst.[16] The addition of dichlorosilane **11** to a suspension of 1,4-dilithiotetraphenylbutadiene in diethyl ether afforded silole **12** in a yield of 38.5%. Compounds **10** and **12** are greenish yellow, air-stable crystalline solids that could be separated by column chromatography on silica gel by using a mixture of hexane/acetone as the eluents (hexane/acetone = 10:1, $R_f$ = 0.36 for **10**; hexane/acetone = 20:1, $R_f$ = 0.51 for **12**) (Scheme 4).

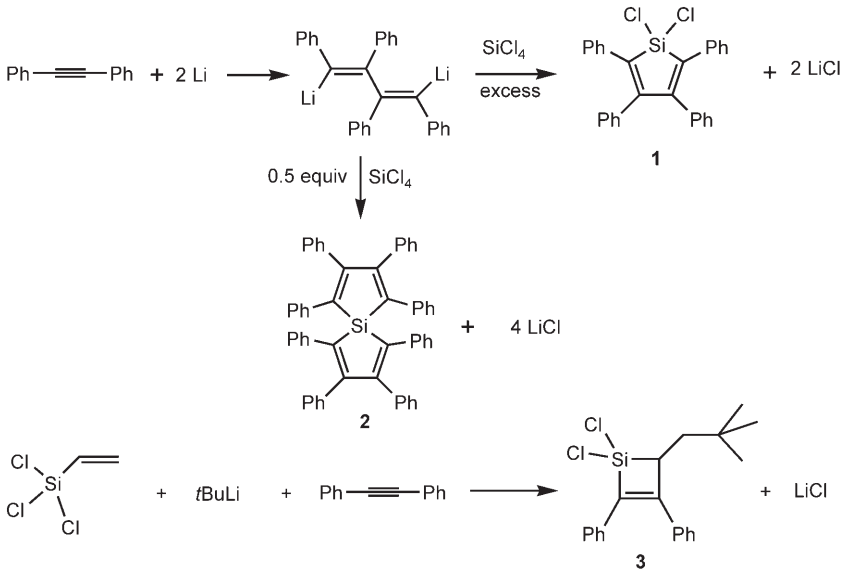


Scheme 1.

**Characterization of compounds 2, 6, 7, 10, and 12**: The unequivocal characterization of

  

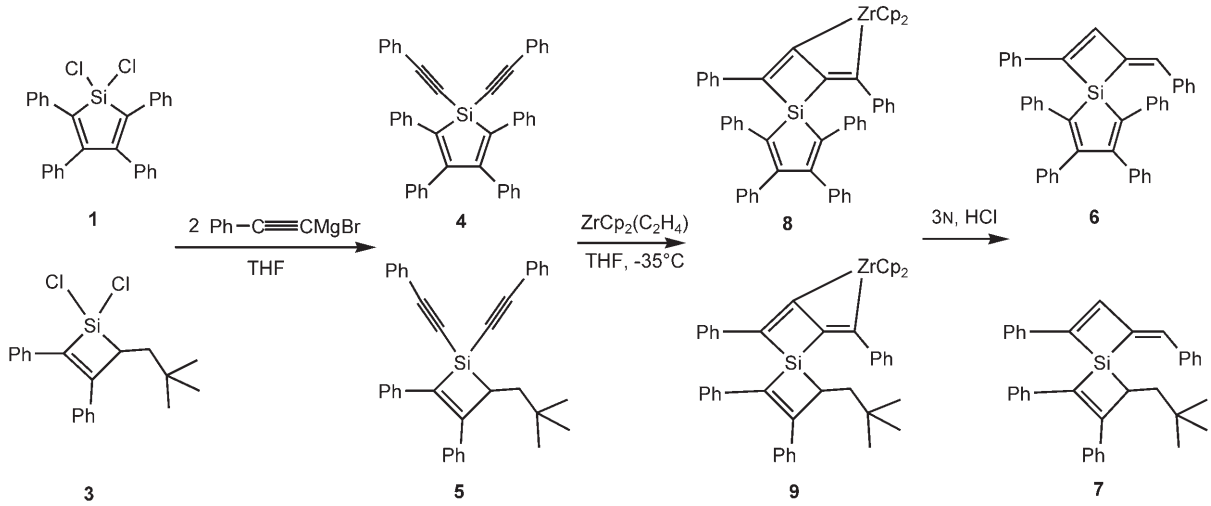


Scheme 2.

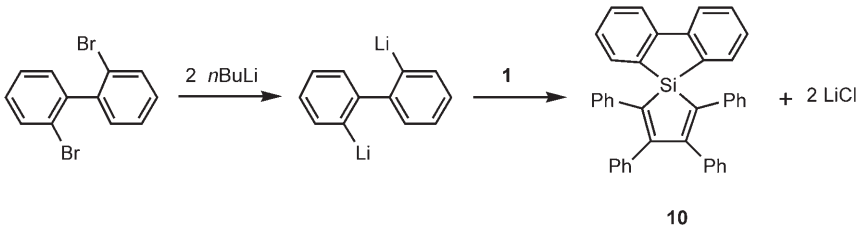


Scheme 3.

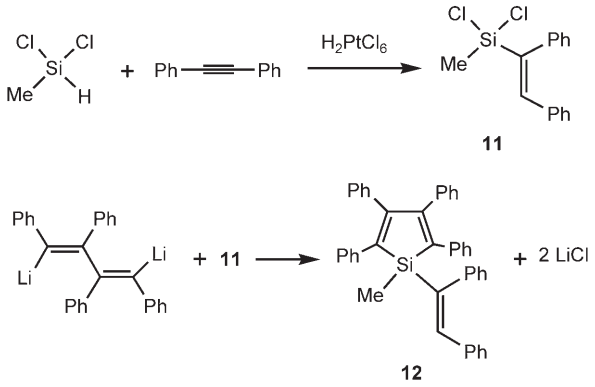


Scheme 4.

compounds **6**, **7**, **10**, and **12** was achieved by means of elemental analysis and standard spectroscopic techniques. In agreement with their molecular structures, the $^{1}H$ and $^{13}C$ NMR spectra of **6**, **7**, **10**, and **12** revealed the presence of silole and silacyclobutene rings. The $^{1}H$ NMR spectra of **6** and **7** have two singlets at $\delta = 8.14$ and 7.00 ppm for **6** and $\delta = 8.11$ and 7.03 ppm for **7**, which were assigned as the PhC*H*=C and −C*H*=C(Ph)Si hydrogen atoms, respectively.[15a] The $^{13}C$ NMR spectra of these compounds show two methine carbon atoms at $\delta = 154.28$ and 130.96 ppm for **6** and $\delta = 153.28$ and 131.16 ppm for **7**, which correspond to the Ph*C*H= carbon atom and a ring carbon atom (−*C*H=C), respectively. These characteristic data are in reasonable agreement with those reported for silacyclobutenes.[15b,17] The most relevant structural data for **2**, **10**, and **12** arise from the characteristic low-field resonances between $\delta = 149$ and 157 ppm for the β-carbon atoms within the silole rings.[4b] The molecular structures were further confirmed by the results of single-crystal X-ray structural analyses of **2**, **6**, **7**, and **12**. Suitable single crystals of **7** were obtained from ethanol and crystals of **6** were obtained by slow diffusion of *n*-hexane into a solution of **6** in diethyl ether. The molecular structures of silaspirenes **6** and **7** were determined at 173 and 140 K, respectively, and are depicted by the ORTEP drawings in Figures 1 and 2. The crystal parameters, data collection parameters, and conditions for structure refinement are summarized in Table 1. Analysis of **6** confirms the existence of both a silole and a silacyclobutene ring with three endocyclic and one exocyclic localized double bonds. The silacyclobutene subunit is perfectly planar (the largest deviation from the plane is 0.0006 Å) and almost perpendicular (86.8°) to the plane of the five-membered ring (largest deviation = 0.0224 Å) in the silole moiety. The four phenyl substituents at the silole ring skeleton show a propeller-like arrangement, the two phenyl rings at the PBSE unit lie within the silacyclobutene plane (interplanar angles = 6.9 and 5.4°). The endocyclic C-Si-C angles within the silole and silacyclobutene rings are 93.08(9) and 74.35°(10), respectively. The molecular structure of the silole unit in **6** is similar to that reported for a silaspirotropylidene, which is a spirocyclic compound that consists of a silole and a silacycloheptene unit.[18] Compared with [{Zr($CH_3C_5H_4$)$_2$}-($C_6H_5$)$_2$Si$C_4$($C_6H_5$)$_2$], a compound in which a zirconocene

  

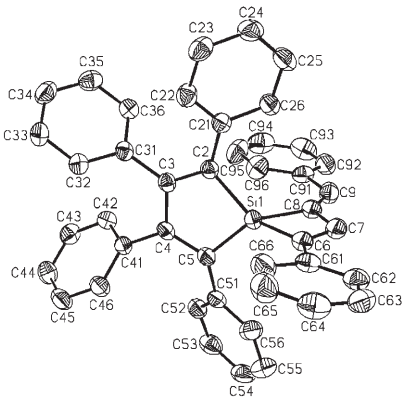


Figure 1. Molecular Structure of **6**. Ellipsoids are drawn at 50% probability. Hydrogen atoms are omitted for clarity. Selected bond lengths [Å] and angles [°]: Si1–C2 1.871(2), Si1–C5 1.874(2), Si1–C6 1.888(2), Si1–C8 1.888(2), C2–C3 1.357(3), C3–C4 1.515(3), C4–C5 1.360(3), C6–C7 1.343(3), C7–C8 1.452(3), C8–C9 1.332(3); C2-Si1-C5 93.08(9), C6-Si1-C8 74.35(10), Si1-C2-C3 107.14(14), Si1-C5-C4 107.06(14), C2-C3-C4 116.39(17), C3-C4-C5 116.19(17), Si1-C6-C7 89.68(15), Si1-C8-C7 86.55(14), C6-C7-C8 109.4(2), C7-C8-C9 130.4(2).

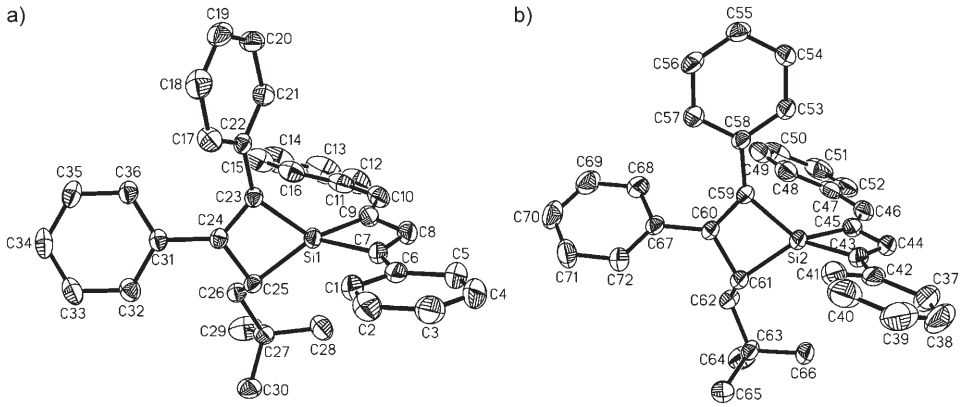


Figure 2. Molecular structure of **7**. Ellipsoids are drawn at 50% probability. Hydrogen atoms are omitted for clarity. Selected bond lengths [Å] and angles [°]: Si1–C7 1.871(2), Si1–C9 1.892(2), Si1–C23 1.852(2), Si1–C25 1.904(2), C7–C8 1.363(3), C8–C9 1.460(3), C9–C10 1.340(3), C23–C24 1.359(2), C24–C25 1.545(2), Si2–C43 1.875(2), Si2–C45 1.893(2), Si2–C59 1.845(2), Si2–C61 1.902(2), C43–C44 1.361(3), C44–C45 1.468(3), C45–C46 1.327(4), C59–C60 1.359(3), C60–C61 1.544(2); C7-Si1-C9 74.83(9), C23-Si1-C25 77.64(7), Si1-C7-C8 90.4(1), C7-C8-C9 108.1(2), Si1-C9-C8 86.7(1), C8-C9-C10 129.1(2), Si1-C23-C24 90.7(1), C23-C24-C25 108.1(1), Si1-C25-C24 83.5(1), C43-Si2-C45 74.9(1), C59-Si2-C61 77.50(8), Si2-C43-C44 90.3(2), C43-C44-C45 108.2(2), Si2-C45-C44 86.5(2), C44-C45-C46 128.1(2), Si2-C59-C60 91.0(1), C59-C60-C61 107.7(1), Si2-C61-C60 83.5(1).

fragment is bound to a silacyclobutene,[15b] the bond lengths C6–C7 (1.343(3) Å) and C8–C9 (1.332(3) Å) in **6** are not significantly different from those in the zirconocene complex (1.348 and 1.322 Å). In contrast, the bond length C7–C8 (1.452(3) Å) in **6** is much shorter than the corresponding carbon–carbon bond of the zirconocene complex (1.595 Å). Whereas the two bond lengths Si1–C6 and Si1–C8 are equal in **6** (1.888 Å, within the expected accuracy), they are different in the zirconocene compound (1.887 and 1.854 Å).[15b]

X-ray structural analysis of silaspirene **7** shows two crystallographically independent molecules (Figure 2). The two silacyclobutene rings in representation a are planar and the angle between the planes is 93.1°, whereas the corresponding moieties in representation b show a small deviation from planarity (the angle between the [C43, Si2, C45] and [C43, C44, C45] planes is 0.07°, and the angle between the [C43, Si2, C45] and [C59, C60, C61] planes is 0.15°) and the interplanar angle between the best planes of the silacyclobutene rings is 88.3°. The two phenyl substituents on the PBSE skeleton are almost coplanar with the silacyclobutene plane (interplanar angles = 7.4 and 22.2° for representation a, and 15.1 and 21.1° for representation b). In the PBSE moiety, the C=C endocyclic double bonds (1.363(3) in representation a and 1.361(3) Å in representation b) are longer than the exocyclic double bonds (1.340(3) in representation a and 1.327(4) Å in representation b), which is similar to the values reported by Rosenthal et al for the metal complex.[10] The two phenyl substituents on the DNSE unit are characterized by very different orientations. They show interplanar angles with the attached silacyclobutene moiety of 52.0 and 34.8° for representation a and 19.5 and 54.2° for representation b. The Si–C bond lengths range from 1.845(2) to 1.904(2) Å and are typical silicon–carbon single bonds. The C-Si-C angles are 74.9° within the PBSE and 77.6° within the DNSE subunit.

The molecular structure of **10** is depicted in Figure 3 with selected bond lengths and angles. The crystal parameters, data collection parameters, and conditions for structure refinement are summarized in Table 1. The single-crystal X-ray analysis was solved in the space group $P2_1/c$, which contained two molecules of **10** and formally 0.5 molecules of acetone in the asymmetric unit. As the two molecular structures look very similar only one of them is shown in Figure 3. The crystal structure reveals that the atoms of the silafluorene unit are coplanar (largest deviation = 0.043 Å), and this plane is almost perpendicular (88.9°) to the silole ring. The silole subunit of **10** shows a typical silole configuration[19] and is similar to the silole moieties in compounds **6** and **12**. The structure of the silafluorene unit is almost comparable with that of diphenylsilafluorene[20a] and spirosilafluorene,[20b] but shows some small differences to that of dichlorosilafluorene.[20c]

X-ray diffraction data of compound **12** were collected at 173 K. Its molecular structure is depicted in Figure 4 and the crystal parameters, data collection parameters, and conditions for structure refinement are summarized in Table 1. The molecular features of the silole subunit of **12** are comparable to those of compound **6**, which itself also shows a

  

Table 1. Crystal data and conditions for crystallographic data collection and structure refinement of **2**, **6**, **7**, **10**, and **12**.[a]

| | **2** | **6** | **7** | **10** | **12** |
|---|---|---|---|---|---|
| formula | $C_{56}H_{40}Si$ | $C_{44}H_{32}Si$ | $C_{36}H_{34}Si$ | $C_{40.75}H_{29.50}O_{0.25}Si$ | $C_{43}H_{34}Si$ |
| $M_r$ | 740.97 | 588.79 | 494.72 | 551.23 | 578.79 |
| color | greenish yellow, transparent | greenish yellow, transparent | colorless, transparent | greenish yellow, transparent | greenish yellow, transparent |
| crystal system | orthorhombic | monoclinic | orthorhombic | monoclinic | triclinic |
| space group | $P2_12_12_1$ | $P2_1/c$ | $P2_12_12_1$ | $P2_1/c$ | $P\bar{1}$ |
| lattice constants | | | | | |
| $a$ [Å] | 10.2326(5) | 10.2196(8) | 10.7021(10) | 10.3957(11) | 10.7261(9) |
| $b$ [Å] | 10.2555(5) | 10.1621(7) | 13.5982(11) | 23.101(2) | 12.3330(10) |
| $c$ [Å] | 38.881(2) | 31.467(2) | 39.147(4) | 26.615(2) | 13.661(2) |
| $\alpha$ [°] | 90 | 90 | 90 | 90 | 80.784(5) |
| $\beta$ [°] | 90 | 95.400(6) | 90 | 93.507(8) | 69.178(6) |
| $\gamma$ [°] | 90 | 90 | 90 | 90 | 72.048(5) |
| $V$ [Å$^3$] | 4080.2(4) | 3253.4(4) | 5697.0(9) | 6379.7(10) | 1604.3(3) |
| $Z$ | 4 | 4 | 8 | 8 | 2 |
| $\rho_{calcd}$ [g cm$^{-3}$] | 1.206 | 1.202 | 1.154 | 1.148 | 1.198 |
| $\mu$ [cm$^{-1}$] | 0.096 | 0.103 | 0.105 | 0.101 | 0.103 |
| radiation | $Mo_{K\alpha}$ | $Mo_{K\alpha}$ | $Mo_{K\alpha}$ | $Mo_{K\alpha}$ | $Mo_{K\alpha}$ |
| monochromator | graphite | graphite | graphite | graphite | graphite |
| $2\theta$ range [°] | $2.05 \le 2\theta \le 25.06$ | $4.22 \le 2\theta \le 52.04$ | $3.18 \le 2\theta \le 65.16$ | $4.92 \le 2\theta \le 50.72$ | $3.2 \le 2\theta \le 59.72$ |
| | $-12 \le h \le 10$ | $-12 \le h \le 12$ | $-15 \le h \le 15$ | $-12 \le h \le 12$ | $-14 \le h \le 14$ |
| | $-11 \le k \le 12$ | $-12 \le k \le 11$ | $-20 \le k \le 19$ | $-27 \le k \le 23$ | $-15 \le k \le 16$ |
| | $-46 \le l \le 46$ | $-38 \le l \le 38$ | $-59 \le l \le 58$ | $-31 \le l \le 31$ | $-17 \le l \le 18$ |
| refl. measured | 30376 | 27854 | 98308 | 32222 | 33523 |
| refl. independent | 7191 | 6361 | 19206 | 11395 | 7953 |
| $R_{int}$ | 0.0586 | 0.035 | 0.046 | 0.0871 | 0.0228 |
| $T$ [K] | 173 | 173 | 140 | 173 | 173 |
| no. of parameters | 515 | 406 | 675 | 755 | 397 |
| $wR2$ | 0.0830 | 0.113 | 0.134 | 0.1735 | 0.1075 |
| $R1$ | 0.0468 | 0.075 | 0.082 | 0.1147 | 0.0485 |
| $R1$ [$F_0 > 4\sigma(F_0)$] | 0.0317 | 0.056 | 0.062 | 0.0604 | 0.0413 |
| max. and min. in $\Delta\sigma$ [e A$^{-3}$] | 0.177, −0.168 | 0.52, −0.30 | 0.90, −0.45 | 1.088, −0.268 | 0.314, −0.297 |

[a] Structure determination: Si positional parameters from direct methods (SHELX-97),[26a] further atoms and refinement from ΔF synthesis (SHELX-97),[26b] refinement by anisotropic full-matrix least-squares procedure for all non-hydrogens, hydrogen position refinement by "riding" model; atomic scattering factors from literature.[26c] An image plate diffractometer system (STOE) was used. Lorenz and polarization coefficient corrections were applied.

typical silole configuration.[19] The stilbene substituent, the methyl group, and the silicon atom form a [C1, Si1, C6, C7] plane (largest deviation = 0.036 Å), which is almost perpendicular (87.6°) to the silole ring. The phenyl carbon atoms C61 (deviation = 0.068 Å) and C71 (deviation = 0.015 Å) are also in this plane. These structural findings are similar to the arrangements of the silacyclobutene and stilbene subunits in DNSE. As attempts to synthesize a DNSE molecule that contains a silole group have been unsuccessful to date, **12** was used as an alternative model compound to investigate its photoluminescence properties. The C6-Si1-C1 angle is much larger than in DNSE (112.5 vs. 77.6° in DNSE) because C1 and C7 are not directly connected. The bond lengths of Si1–C6 (1.85 Å) and Si1–C1 (1.88 Å) are similar to those in DNSE (1.84 and 1.90 Å, respectively). The two phenyl rings in the stilbene moiety have different orientations. Their interplanar angles with the [C1, Si1, C6, C7] plane are 78.0 and 22.2°, respectively.

Finally, the structure of the "pure" silole spiro compound **2** was determined by single-crystal X-ray diffraction analysis. An ORTEP plot of **2** is shown in Figure 5 and crystallographic information is summarized in Table 1. The Si–C bond lengths are analogous to those of the Si–C bond in **6** and are in the typical bond length range of siloles.[19] According to the crystallographic data, the silole rings are perpendicular (the angle between the [C4, Si1, C1] and [C8, Si1, C5] planes is 89.9°).

**Investigation of the optoelectronic properties of compounds 2, 4–7, 10, and 12–14**: The monocyclic building blocks of the silaspirenes, such as siloles **4** and **13** and silacyclobutenes **5** and **14**, exhibit intense photoluminescence upon excitation with UV light.[21] In general, the silole luminescence is due to a σ*–π* LUMO that is stabilized through the conjugation of the σ* orbital of the two exosilole silicon–carbon bonds with the π* orbital of the butadiene moiety.[22] For the characteristic photoluminescence properties of silacyclobutenes it is mainly the stilbene subunit that is responsible.[23] The UV-visible spectra and the photoluminescence of bicyclic silaspirenes **2**, **6**, **7**, and **10** were measured in solution and also in the solid state and compared with data obtained for monocyclic compounds **4**, **5**, **13**, and **14**.

As the stilbene subunit is responsible for the intense blue photoluminescence of ring compound **5**,[4d,23] compound **12**, which contains a silole ring and an exocyclic stilbene subunit, has also been included in our investigations for comparison. Important optophotoelectronic features were extracted from the spectra and are listed in Table 2. The UV-visible spectra of both silaspirenes **6** and **7** show a strong absorption band at 300 to 370 nm, which is similar to that of monocycle **14** with respect to the maxima, vibration structures, and appearances. Therefore, the absorption has been assigned to the π–π* transition of the butadiene moieties of the PBSE subunits.[4d] Clearly the silole and DNSE rings have no significant influence on these absorptions, but for both silaspirenes the extinction coefficient ($\varepsilon$) decreases compared with respect to the $\varepsilon$ detected for compound **14**.

  

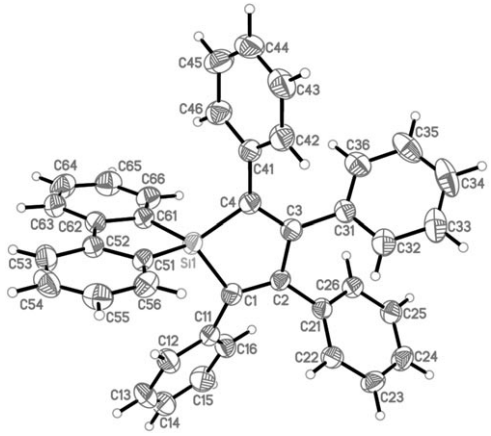


Figure 3. Molecular structure of **10**. Ellipsoids are drawn at 50% probability. Selected bond lengths [Å] and angles [°]: Si1−C1 1.868(3), Si1−C4 1.865(4), Si1−C51 1.865(4), Si1−C61 1.862(4), C1−C2 1.352(5), C2−C3 1.521(5), C3−C4 1.358(5), C51−C52 1.419(5), C61−C62 1.409(5), C52−C62 1.476(5), C51−C56 1.398(5), C61−C66 1.401(5), C55−C56 1.388(5), C65−C66 1.388(6), C54−C55 1.388(6), C64−C65 1.377(6), C53−C54 1.381(6), C63−C64 1.385(6), C52−C53 1.395(5), C62−C63 1.391(5); C1-Si1-C4 92.71(15), C51-Si1-C61 92.00(16), C2-C1-Si1 107.9(2), C1-C2-C3 115.7(3), C2-C3-C4 115.9(3), C3-C4-Si1 107.7(2), C52-C51-Si1 108.5(3), C51-C52-C62 115.3(3), C62-C61-Si1 109.1(3), C61-C62-C52 115.1(3).

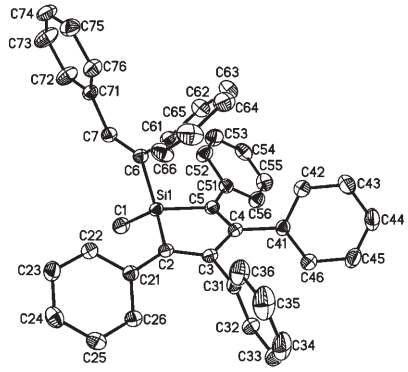


Figure 4. Molecular Structure of **12**. Ellipsoids are drawn at 50% probability. Hydrogen atoms are omitted for clarity. Selected bond lengths [Å] and angles [°]: Si1−C1 1.8581(12), Si1−C2 1.8702(11), Si1−C5 1.8682(12), Si1−C6 1.8812(12), C2−C3 1.3612(15), C3−C4 1.5089(16), C4−C5 1.3639(15), C6−C7 1.3455(16), C6−C61, 1.4966(15), C7−C71 1.4769(16); C1-Si1-C6 112.51(5), C2-Si1-C5 92.63(5), C7-C6-Si1 119.85(9), C7-C6-C61 124.01(10), C6-C7-C71 130.90(11).

Whereas a weak absorption band at about 400 nm has been found for **6** and assigned to the absorption of the silole moiety, no band originating from the DNSE moiety could be detected in the spectrum of **7**. The absorption spectra for compounds **2**, **10**, and **12** also have an absorption band in the near-UV range (300–380 nm), which mainly originates from the silole rings. Compared to the absorption of diethynylsilole **4** at 374 nm, spirosilole **10** has a similar absorption peak position (379 nm) with a slight increase of the extinction coefficient; this is assumed to arise from a small contribution of the silafluorene unit because diphenylsilafluorene

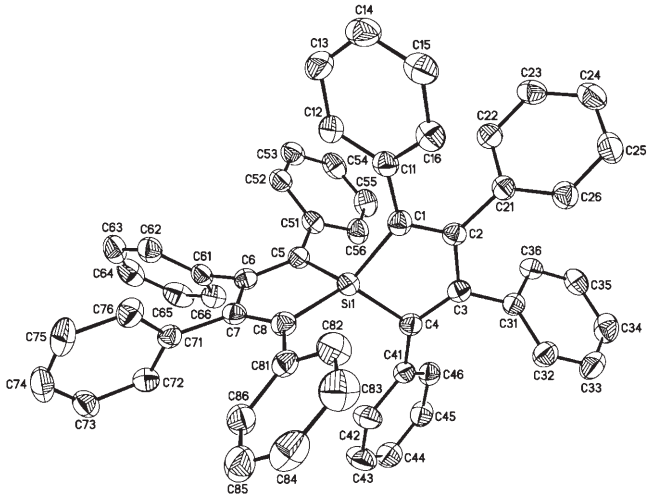


Figure 5. Molecular structure of **2**. Ellipsoids are drawn at 50% probability. Hydrogen atoms are omitted for clarity. Si1−C1 1.874(2), Si1−C4 1.887(2), C1−C2 1.364(3), C2−C3 1.502(3), C3−C4 1.366(3), C1−C11 1.475(3), C2−C21 1.494(3); C1-Si1-C4 92.77(9), Si1-C1-C2 106.49(15), C1-C2-C3 117.02(17), C2-C3-C4 116.08(17), C3-C4-Si1 106.76(15), C1-Si1-C5 113.84(9), C1-Si1-C8 123.95(9).

**13** shows a weak absorption at 321 nm. The near-UV absorption peak of "unspiro" silole **12** is blueshifted 10 nm compared with spirosilole **10** and the extinction coefficient is further increased to $1.24\times10^4\,mol^{-1}cm^{-1}$. Spirosilole **2**, which contains two tetraphenyl-silacyclopentadiene units, has absorption positions similar to diethynylsilole **4** and spirosilole **10**, but the extinction coefficient of **2** is about twice as high as that of **4**. This difference is owing to the fact that **2** con-

Table 2. Absorption and emission data of compounds **2**, **4**–**7**, and **10**, **12**–**15**.[a]

| Compd | UV | | Fluorescence (s)[b] | Fluorescence (THF)[c] |
|---|---|---|---|---|
| | $\lambda_{max}$ [nm] | $\varepsilon$ [$\times10^4$] | $\lambda_{em}$ ($\lambda_{ex}$)[d] [nm] | $\lambda_{em}$ ($\lambda_{ex}$)[d] [nm] |
| **2** | 378 | 2.10 | 504 (393) | 510 (393) |
| **4** | 374 | 0.99 | | |
| | 253 | 7.34 | 500 (452, 393) | 495 (388) |
| | 210 | 9.1 | | |
| **5** | 267 | 7.01 | | |
| | 257 | 7.84 | 384 (313) | 370 (303) |
| | 210 | 9.8 | | |
| **6** | 340 | 3.8 | 510 (300, 234) | 388 (296, 341) |
| | 353 | 3.9 | 410 (234) | 503 (341) |
| **7** | 338 | 2.7 | 438 (260–392) | 416 (345, 280) |
| | 351 | 2.6 | | |
| **10** | 379 | 1.11 | 499 (393) | 386, 503 (320) |
| **12** | 369 | 1.24 | 510 (393) | 374, 490 (300) |
| **13** | 321 | 0.08 | | |
| **14** | 339 | 4.08 | 450 (394) | 406 (346) |
| | 351 | 4.07 | | |
| **15** | | | | 416 (345, 280) |
| | | | | 330 (228, 280) |
| | | | | 310 (280) |

[a] $\lambda_{ex}$ is the excitation wavelength and $\lambda_{em}$ is the emission wavelength. [b] Fluorescence measurement of sample in the solid state. [c] Fluorescence measurement of solutions of the sample in THF. [d] Excitation wavelengths are given in parentheses.

  

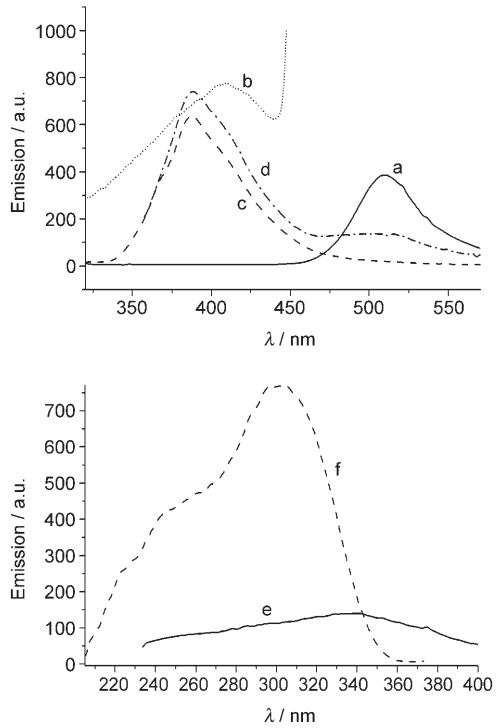


Figure 6. Photoluminescence spectra of silaspirene **6** ($\lambda_{ex}$ is the excited wavelength). a) Solid-state emission spectrum ($\lambda_{ex}=300$ nm), b) amplified solid-state emission spectrum ($\lambda_{ex}=234$ nm), c) emission spectrum of a solution in THF ($\lambda_{ex}=296$ nm), d) emission spectrum of a solution in THF ($\lambda_{ex}=341$ nm), e) excitation spectrum of a solution in THF ($\lambda_{fixed}=503$ nm), and f) excitation spectrum of a solution in THF ($\lambda_{fixed}=387$ nm).

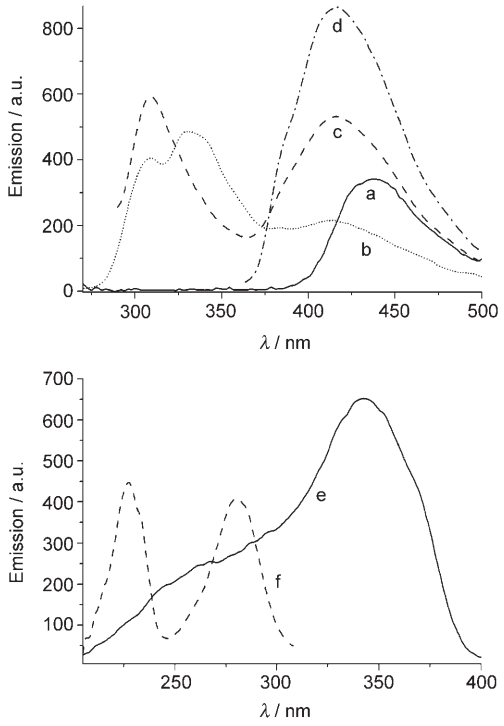


Figure 7. Photoluminescence spectra of silaspirene **7** and its photoreaction product **15**. a) Solid-state emission spectrum of **7** ($\lambda_{ex}=260$ nm), b) emission spectrum of a solution of silaspirene **15** in THF ($\lambda_{ex}=228$ nm), c) emission spectrum of a solution of **15** in THF ($\lambda_{ex}=280$ nm), d) emission spectrum of a solution of **15** in THF ($\lambda_{ex}=344$ nm), e) excitation spectrum of a solution of **15** in THF ($\lambda_{fixed}=416$ nm), and f) excitation spectrum of a solution of **15** in THF ($\lambda_{fixed}=325$ nm).

sists of two silole rings within each molecule, whereas **4** has only one silole ring. Moreover, data comparison reflects the fact that the phenylacetylide substituents in **4** have no remarkable influence on the optical properties of the compound.

As illustrated in Figures 6 and 7, the fluorescence behavior of silaspirenes **6** and **7** is complicated and depends strongly on the excitation wavelength and state of the sample used. Upon excitation at 300 nm, a powder sample of **6** exhibited a strong emission band at 510 nm, which corresponds to the typical emission of a silole (Figure 6a).[4] However, when the excitation wavelength was fixed at 234 nm and the emission spectrum was amplified then a small band was observed at 410 nm that corresponds to the emission of a PBSE subunit (Figure 6b). When the spectrum was recorded as a solution of **6** in THF then the PBSE emission at 388 nm becomes predominant (Figure 6c). When the solution was excited at 341 nm then a small band that resulted from the silole unit was observed at around 500 nm (Figure 6d). This phenomenon is in close agreement with the low photoluminescence of solutions of siloles in THF that have been reported.[21]

The emission spectrum of silaspiroheptene **7** in the solid state (Figure 7a) was quite simple and contained only one broad band at 438 nm that originated from the conjugated butadiene system of the PBSE unit. No bands resulting from the DNSE moiety could be assigned. In contrast, the fluorescence of a solution of **7** in THF is rather complicated. At first, only an emission at around 416 nm that originated from the PBSE unit was observed. With exposition to UV light, an emission between $\lambda=310$ and 335 nm appears rapidly and its intensity increases with time. This behavior is typical for solutions of 2,3-diphenyl-3-neopentyl-1-silacyclobut-2-enes in THF, and results from the photochemical reaction depicted in Scheme 5.[23]

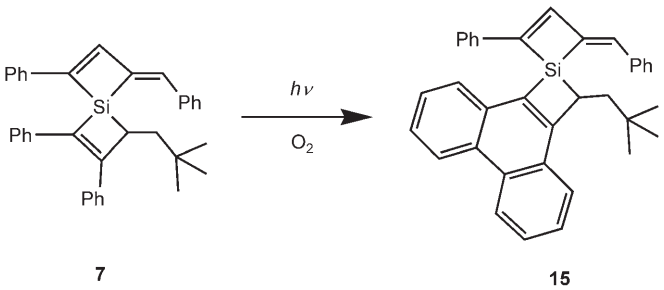


Scheme 5.

Upon excitation of the solution of **15** in THF at 228 nm, the predominant emission is detected as a broad band between 300 and 360 nm that results from the phenanthrene

  

moiety (Figure 7b). Excitation at 344 nm causes the appearance of a single strong broad band at 416 nm, which is attributed to the PBSE part (Figure 7d). When an excitation wavelength of 280 nm was used, both emission bands (344 and 416 nm) were detected (Figure 7c).

The excitation spectra of silaspirenes **6** and **15** also exhibit interesting properties and are highly dependent on the emission wavelength. When the emission is fixed at the wavelength of the silole (503 nm) or the PBSE bands (**6**: 387 nm; **7**: 416 nm), the excitation spectra resemble those of the silole (Figure 6e) and PBSE monomers (**6**: Figure 6f, **7**: Figure 7e), respectively.[4d] However, when the emission is fixed at the wavelength of the phenanthrene moiety absorption (325 nm), the excitation spectrum has two peaks (Figure 7f), which is different from that of its corresponding cyclomonomer (broad band, 240–340 nm).[4d] The reason for this phenomenon is still under investigation.

The excitation of a solution of spiro compound **10** in THF by UV light in the range of 255 to 345 nm resulted in two emission bands as shown in Figure 8a. The low energy emission at 503 nm originates from the silole moiety and the one at 386 nm stems from the silafluorene unit. The excitation spectra of **10** (Figure 8b and c) revealed that the relative emission intensities of the two peaks at 386 nm and 503 nm were highly dependent on the excitation UV wavelength. In the range from 312 to 344 nm, the silafluorene emission is stronger than that of the silole, whereas for other wavelengths (<312 nm or >344 nm) the silole emission is stronger. At wavelengths longer than 355 nm, the energy of the incident light is not sufficient to excite the emission at 386 nm and only one emission at 503 nm remains. Emissions from both silole and silafluorene moieties are weak for a solution in THF. Siloles usually show weak emissions in organic solutions owing to the quenching effect caused by the rotation of the phenyl groups situated at the butadiene ring.[21] The weak emission of silafluorene is partially due to its low near-UV absorption (Table 2). These results also reveal the relatively independent optoelectronic properties of the two silaorganic unsaturated rings. The silole absorption contributes to the silole emission and the silafluorene absorption affords the silafluorene emission, but no evidence for any exchange of energy between the two rings was observed. The emission of spiro compound **10** in the solid state is quite simple, only one strong green emission at 499 nm is detected (Figure 8d), which shows the typical emission properties of a silole. Compared with the strong emission of a silole, the emission of the silafluorene is too weak to be observed.

The photoluminescence spectra of "unspiro" compound **12** are depicted in Figure 9. A comparison of the spectra of **10** (Figure 8) and **12** (Figure 9) reveals that the photoluminescent properties of both compounds are similar in many aspects. The solution of **12** in THF exhibits two emission bands at 490 and 374 nm (Figure 9b) that originate from the silole ring and stilbene moiety, respectively. By using an excitation wavelength beyond 353 nm, only a low-energy emission band from the silole at 490 nm is observed. Both emissions of the silole and stilbene subunits are very weak. In the solid state only a strong green emission from the silole moiety is detected. There are also some differences in the spectra. Spiro compound **10** shows a slight blue shift (from 503 to 499 nm, see Table 2) when comparing the emission of a solution in THF and the solid state, whereas **12** reveals a moderate red shift (from 490 to 510 nm, Table 2).

In contrast to the stilbene moiety in **7**, that of **12** reacts extremely slowly to form a phenanthrene subunit upon irra-

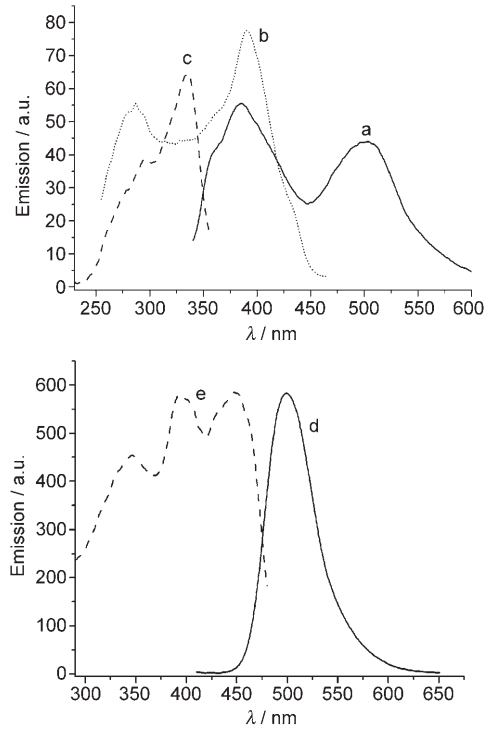


Figure 8. Photoluminescence spectra of silole **10**. a) Emission spectrum of a solution in THF ($\lambda_{ex}=320$ nm), b) excitation spectrum of a solution in THF ($\lambda_{fixed}=500$ nm), c) excitation spectrum of a solution in THF ($\lambda_{fixed}=386$ nm), d) solid-state emission spectrum ($\lambda_{ex}=393$ nm), and e) solid-state excitation spectrum ($\lambda_{fixed}=499$ nm).

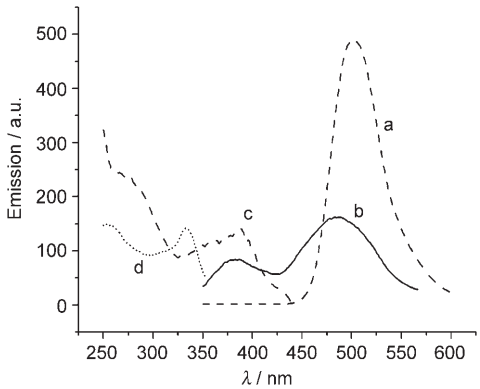


Figure 9. Emission and excitation spectra of **12**. a) Solid-state emission spectrum ($\lambda_{ex}=310$ nm) b) emission spectrum of a solution in THF ($\lambda_{ex}=300$ nm), c) excitation spectrum of a solution in THF ($\lambda_{fixed}=490$ nm), and d) excitation spectrum of a solution in THF ($\lambda_{fixed}=374$ nm).

  

diation with UV light in the presence of oxygen. This different reaction pattern is understandable when considering that the stilbene unit in **12** isomerizes to form *trans*-stilbene,[25a,b] thus reducing the efficiency of forming an intramolecular phenanthrene moiety. In contrast, this stilbene *cis*/*trans* isomerization is not possible for **7**, which allows a rapid reaction to occur (Scheme 5). Furthermore, there are probably steric interactions between the silole units and the phenyl rings of the stilbenes that prohibit the suitable orientation of the phenyl rings for the reaction, namely, the coplanar conformation of the phenyl rings with the olefinic unit.[25c]

The photoluminescence properties of spirosilole **2** has similar properties to those discussed for siloles and the results of the optoelectronic investigations are shown in Figure 10. The main difference is the emission intensity of compound **2** in the solid state, which is lower than that observed for most monocyclic siloles.

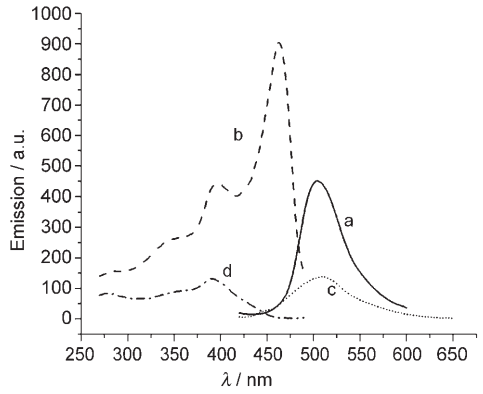


Figure 10. Emission and excitation spectra of **2**. a) Solid-state emission spectrum ($\lambda_{ex}=393$ nm), b) solid-state excitation spectrum ($\lambda_{fixed}=510$ nm), c) emission spectrum of a solution in THF ($\lambda_{ex}=393$ nm), and d) excitation spectrum of a solution in THF ($\lambda_{fixed}=510$ nm).

## Conclusions

A series of organo functional substituted derivatives (**4**, **5**, and **14**) and spiro compounds (**2**, **6**, **7**, and **10**) were synthesized from silicon dichloro substituted silole **1** and silacyclobutene **3**. All of the compounds discussed have interesting optoelectronic properties, which might be used for the design of new LED and/or sensor materials, and are based on both a strong blue photoluminescence of the solid-state materials and their ability to show different emission maxima depending on the state of the sample and the excitation wavelengths used. These compounds can be introduced into polymeric backbones of carbosilanes, polysilanes, and siloxanes by using functional groups at the silicon center or by using suitable ring-opening polymerization reactions, thus transferring the photoluminescent properties into new materials with promising optoelectronic properties. These investigations are now being performed in our laboratories. Thus, linking the photoluminescent silicon-based building blocks into conjugated π systems improves the luminescent properties of the new materials that are obtained.

## Experimental Section

**General procedures**: All reactions were carried out under an argon atmosphere (99.99%, Messer-Griesheim) by using standard Schlenk techniques. Solvents were purified by using standard methods and distilled under argon prior to use. Literature methods were used to prepare dichlorosilanes **1**,[11] **3**,[13] and **11**;[16] silole **2**;[12] silacyclobutene **5**;[14,4d] and silafluorene **13**.[24] All other reactant compounds were commercially available. NMR spectra were obtained by using a Bruker DPX 250 spectrometer ($^1$H NMR, 250 MHz; $^{13}$C NMR, 62.9 MHz; $^{29}$Si NMR, 49.7 MHz). Chemical shifts are reported in ppm with reference to the $CDCl_3$ peak for $^{13}$C NMR spectroscopy and the TMS peak for $^1$H and $^{29}$Si NMR spectroscopy. UV-visible and fluorescence spectra were recorded by using a CARY-1 UV/Vis spectrophotometer and a Perkin–Elmer LS 50B luminescence spectrometer, respectively. Microanalyses were performed by using a Foss Heraeus CHN-O-RAPIO instrument.

**Synthesis of 4 and 5**: A solution of PhC≡CMgBr (50 mmol) in THF (50 mL) was added dropwise to a solution of **1** (10.5 g, 23.1 mmol) in THF (20 mL) at room temperature. The reaction mixture was stirred at room temperature for 1 h before ice was added. The resulting mixture was extracted with diethyl ether (3×100 mL) and washed with water and brine. The extract was dried over $MgSO_4$ and the solvent was removed in vacuo at room temperature to give a yellow solid. Recrystallization from acetone resulted in the formation of **4** as greenish yellow crystals (9.9 g, 73%). $^1$H NMR (250 MHz, $CDCl_3$): $\delta=7.51$–$6.89$ ppm (m, 30H; Ph); $^{13}$C NMR (62.9 MHz, $CDCl_3$): $\delta=156.6$, 138.4, 137.9, 135.0, 132.4, 129.7, 129.5, 129.3, 128.2, 127.9, 127.6, 126.7, 126.2, 122.3, 108.6, 85.7 ppm; $^{29}$Si NMR (49.7 MHz, $CDCl_3$): $\delta=-49.13$ ppm; elemental analysis calcd (%) for $C_{44}H_{30}Si$: C 90.06, H 5.15; found: C 89.62, H 5.19.

Compound **5** was prepared in an analogous procedure to that described for **4** by using 1,1-dichloro-2,3-diphenyl-3-neopentyl-1-silacyclobut-2-ene **3** instead of **1** as a starting material. Compound **5** was isolated as white needles after concentration of the mother liquor (9.7 g, 86%). $^1$H NMR (250 MHz, $CDCl_3$): $\delta=7.55$–$7.07$ (m, 20H; Ph), 2.63 (dd, $^3J=12.4$ Hz, $^3J=4.4$ Hz, 1H; CH), 1.60 (dd, $^3J=12.8$ Hz, $^2J=13.9$ Hz, 1H; $CH_2$), 1.46 (dd, $^3J=4.4$ Hz, $^2J=13.5$ Hz, 1H; $CH_2$), 0.96 ppm (s, 9H; $C(CH_3)_3$); $^{13}$C NMR (62.9 MHz, $CDCl_3$): $\delta=159.4$, 141.4, 136.52, 136.45, 132.3, 132.2, 129.2, 128.33, 128.25, 128.2, 128.1, 127.9, 126.9, 122.4, 122.1, 109.2, 108.3, 87.6, 87.4, 40.9, 31.6, 31.0, 29.7 ppm; $^{29}$Si NMR (49.7 MHz, $CDCl_3$): $\delta=-47.37$ ppm; elemental analysis calcd (%) for $C_{36}H_{32}Si$: C 87.75, H 6.55; found: C 87.51, H 6.66.

**Synthesis of 6**: EtMgBr (1.0 M THF solution, 1.3 mL, 1.3 mmol) was added dropwise to a solution of $[ZrCl_2Cp_2]$ (0.190 g, 0.65 mmol) in THF (10 mL) at −78 °C. After addition was complete, the reaction mixture was stirred at −78 °C for 1 h. Diethynylsilole **4** (0.293 g, 0.50 mmol) was added with stirring at −35 °C and the reaction mixture was stirred for an additional 14 h. Finally, 3 N aqueous HCl (5 mL) was added at room temperature, the reaction mixture was extracted with diethyl ether (3× 70 mL), and washed with water and brine. The extract was dried over $MgSO_4$. The solvent was evaporated in vacuo to give a brown solid that was purified by column chromatography over silica gel ($R_f=0.45$, hexane/ethyl acetate = 10:1) to give **6** (0.076 g, 26%) as greenish yellow crystals. $^1$H NMR (250 MHz, $CDCl_3$): $\delta=8.14$ (s, 1H), 7.51–6.90 ppm (m, 31H); $^{13}$C NMR (62.9 MHz, $CDCl_3$): $\delta=157.1$, 154.8, 154.3, 141.0, 139.0, 138.4, 138.0, 136.5, 134.3, 131.0, 129.7, 129.1, 128.7, 128.5, 128.2, 127.9, 127.7, 127.3, 127.1, 126.74, 126.69, 126.0 ppm; $^{29}$Si NMR (49.7 MHz, $CDCl_3$): $\delta=2.25$ ppm; elemental analysis calcd (%) for $C_{44}H_{32}Si$: C 89.75, H 5.48; found: C 89.65, H 5.62.

**Synthesis of 7**: EtMgBr (1.0 M THF solution, 2.5 mL, 2.5 mmol) was added dropwise to a solution of $[ZrCl_2Cp_2]$ (0.365 g, 1.25 mmol) in THF (15 mL) in a 50 mL Schlenk tube at −78 °C (dry ice/acetone bath). After completion, the reaction mixture was stirred at −78 °C for 1 h. Subse-

  

quently, diethynylsilane **4** (0.493 g, 1.0 mmol) was added and the mixture was allowed to gradually warm up to room temperature and was stirred for an additional hour. 3 N Aqueous HCl (5 mL) was added, the reaction mixture was extracted with diethyl ether (3×70 mL), and the organic phase was washed with water and brine. The extract was dried over $MgSO_4$. The solvent was evaporated in vacuo to give a brown solid. Recrystallization from ethanol afforded colorless crystals of **7** (0.34 g, 69 %). $^1$H NMR (250 MHz, $CDCl_3$): $\delta$ = 8.11 (s, 1H), 7.60–7.11 (m, 20H), 7.03 (s, 1H), 3.08–3.02 (m, 1H), 1.56–1.24 (m, 2H), 0.71 ppm (s, 9H); $^{13}$C NMR (62.9 MHz, $CDCl_3$): $\delta$ = 159.6, 157.8, 153.3, 145.6, 144.3, 139.1, 136.9, 136.8, 136.4, 132.0, 131.2, 128.7, 128.5, 128.4, 128.33, 128.25, 128.12, 128.06, 127.2, 127.12, 127.07, 126.7, 41.1, 34.0, 30.5, 29.1 ppm; $^{29}$Si NMR (49.7 MHz, $CDCl_3$): $\delta$ = −5.14 ppm; elemental analysis calcd (%) for $C_{36}H_{34}Si$: C 87.40, H 6.93; found: C 87.32, H 6.68.

**Synthesis of 10**: 2,2′-Dibromobiphenyl (0.5 g, 1.6 mmol) and dry diethyl ether (20 mL) were placed in a 50 mL Schlenk flask and the mixture was cooled to −78 °C before *n*BuLi (23 % in hexane, ≈2.5 M; 1.5 mL, 3.8 mmol) was added dropwise with constant stirring. After completion, the reaction mixture was warmed up to room temperature and stirred for 20 h to form 2,2′-dilithiumbiphenyl. This solution was added dropwise to a solution of 1,1-dichlorosilole (0.87 g, 1.9 mmol) in diethyl ether (50 mL) at room temperature and stirred for 3 d. Water (10 mL) was added and the organic phase was washed with water (3×20 mL). After drying over $MgSO_4$, the solvent was evaporated in vacuo to give a yellow solid that was purified by column chromatography over silica gel ($R_f$ = 0.36, hexane/acetone = 10:1) to give **10** as a greenish yellow crystalline solid (0.233 g, 26 %). $^1$H NMR (250 MHz, $CDCl_3$): $\delta$ = 7.80–6.59 ppm (m, 28H); $^{13}$C NMR (62.9 MHz, $CDCl_3$): $\delta$ = 158.4, 149.9, 139.0, 138.4, 134.6, 133.9, 132.2, 131.1, 129.9, 129.1, 128.1, 127.71, 127.68, 126.6, 125.8, 121.4 ppm; $^{29}$Si NMR (49.7 MHz, $CDCl_3$): $\delta$ = −0.41 ppm; elemental analysis calcd (%) for $C_{40}H_{28}Si$·0.75acetone: C 87.45, H 5.64; found: C 87.07, H 5.67. Element analysis reveals that there are more acetone molecules in the crystals than those determined by single-crystal X-ray analysis, which only found 0.25 molecules of acetone. This difference is probably because not all of the acetone absorbed by the crystals can be detected by X-ray diffraction.

**Synthesis of 12**: Tolane (5.33 g, 30 mmol), lithium granules (0.28 g, 40 mmol), and dry diethyl ether (20 mL) were placed in a 250 mL Schlenk flask. The mixture was stirred at room temperature under argon for 4 h to give a brown solution and a yellow precipitate. THF (100 mL) was added to dissolve the precipitate to obtain a solution of dilithium tetraphenylbutadiene. This solution was added dropwise to a solution of dichlorosilane **11** (6.83 g, 23.3 mmol) in dry THF (30 mL). Subsequently, the mixture was refluxed for 3 h to obtain a yellow solution that was cooled to room temperature and treated with water (70 mL). The reaction mixture was extracted with diethyl ether (3×70 mL). The organic phase was washed with water and brine and dried over $MgSO_4$. The solvent was removed in vacuo to give a brown solid that was purified by column chromatography over silica gel ($R_f$ = 0.51, hexane/acetone = 20:1) to give **12** as greenish yellow crystals (3.34 g, 38.5 %). $^1$H NMR (250 MHz, $CDCl_3$): $\delta$ = 7.30–6.62 (m, 31H), 0.83 ppm (s, 3H; $CH_3$); $^{13}$C NMR (62.9 MHz, $CDCl_3$): $\delta$ = 156.0, 141.5, 141.1, 140.8, 139.2, 139.0, 138.7, 137.1, 129.6, 129.5, 129.1, 128.0, 127.9, 127.8, 127.6, 127.5, 127.4, 126.1, 126.0, 125.6, −6.89 ppm; $^{29}$Si NMR (49.7 MHz, $CDCl_3$): $\delta$ = 1.46 ppm; elemental analysis calcd (%) for $C_{43}H_{34}Si$: C 89.23, H 5.92; found: C 88.93, H 5.92.

**Crystallographic data**: The supplementary crystallographic data for compounds **2** (CCDC-641076), **6** (CCDC-185864), **7** (CCDC-185855), **10** (CCDC-641075), and **12** (CCDC-641074) can be obtained free of charge from the Cambridge Crystallographic Data Centre via www.ccdc.cam.ac.uk/data_request/cif.

## Acknowledgement

We thank the Deutsche Forschungsgemeinschaft (DFG) for financial support.

[1] a) C. W. Tang, S. A. Vanslyke, *Appl. Phys. Lett.* **1987**, *51*, 913; b) C. W. Tang, S. A. Vanslyke, C. H. Chen, *J. Appl. Phys.* **1989**, *65*, 3610.
[2] C. Adachi, T. Tsutsui, S. Saito, *Appl. Phys. Lett.* **1990**, *57*, 531.
[3] A. Kraft, A. C. Grimsdate, A. B. Holmes, *Angew. Chem.* **1998**, *110*, 416; *Angew. Chem. Int. Ed.* **1998**, *37*, 402.
[4] a) J. Luo, Z. Xie, J. W. Y. Lam, L. Cheng, H. Chen, C. Qiu, H. S. Kwok, X. Zhan, Y. Liu, D. Zhu, B. Z. Tang, *Chem. Commun.* **2001**, 1740; b) J. Chen, C. C. W. Law, J. W. Y. Lam, Y. Dong, S. M. F. Lo, I. D. Williams, D. Zhu, B. Z. Tang, *Chem. Mater.* **2003**, *15*, 1535; c) Y. Ren, J. W. Y. Lam, Y. Dong, B. Z. Tang, K. S. J. Wong, *J. Phys. Chem. B* **2005**, 109, 1135; d) D. Yan, T. Müller, M. Bolte, N. Auner in *Organosilicon Chemistry V: From Molecules to Materials* (Eds.: N. Auner, J. Weis), VCH, Weinheim **2003**, p. 139.
[5] a) P. J. Fagan, W. A. Nugent, *J. Am. Chem. Soc.* **1988**, *110*, 2310; b) J. M. Tour, R. Wu, J. S. Schumm, *J. Am. Chem. Soc.* **1990**, *112*, 5662; c) J. Guay, A. Diaz, R. Wu, J. M. Tour, *J. Am. Chem. Soc.* **1993**, *115*, 1869; d) T. Horn, M. Baumgarten, L. Gerghel, V. Enkelmann, K. Müllen, *Tetrahedron Lett.* **1993**, *34*, 5889.
[6] S. Inoe, H. Kawachi, JP 07188255, **1995**.
[7] a) K. Suzuki, Y. Hashimoto, A. Senoo, K. Ueno, EP 1120839, **2001**; b) T. Kano, T. Shimizu, T. Ogiwara, T. Kaneko, M. Nakajima, H. Kurihara, JP 08119974, **1996**; c) T. Shimizu, T. Kano, T. Ogiwara, T. Kaneko, M. Nakajima, H. Kurihara, JP 08020588, **1996**.
[8] a) S. H. Lee, B. Jang, Z. H. Kafafi, *J. Am. Chem. Soc.* **2005**, *127*, 9071; b) K. Suzuki, Y. Hashimoto, A. Senoo, K. Ueno, EP 1120840, **2001**.
[9] L. C. Palilis, H. Murata, M. Uchida, Z. H. Kafafi, *Org. Electron.* **2003**, *4(2–3)*, 113.
[10] P. M. Pellny, N. Peulecke, V. V. Burlakov, W. Baumann, A. Spannenberg, U. Rosenthal, *Organometallics* **2000**, *19*, 1198.
[11] W. C. Joo, J. H. Hong, S. B. Choi, H. E. Son, C. H. Kim, *J. Organomet. Chem.* **1990**, *391*, 27.
[12] E. H. Braye, W. Hübel, I. Caplier, *J. Am. Chem. Soc.* **1961**, *83*, 4406.
[13] a) N. Auner, C. Seidenschwarz, E. Herdtweck, *Angew. Chem.* **1991**, *103*, 1172; *Angew. Chem. Int. Ed. Engl.* **1991**, *30*, 1151; b) M. Backer, M. Grasmann, W. Ziche, N. Auner, C. Wagner, E. Herdtweck, W. Hiller, M. Heckel in *Organosilicon Chemistry II: From Molecules to Materials* (Eds.: N. Auner, J. Weis), VCH, Weinheim **1996**, p. 41.
[14] M. Backer, PhD Thesis, Humboldt University of Berlin (Germany), **1998**.
[15] a) T. Takahashi, Z. Xi, Y. Obora, N. Suzuki, *J. Am. Chem. Soc.* **1995**, *117*, 2665; b) Z. Xi, R. Fischer, R. Hara, W. H. Sun, Y. Obora, N. Suzuki, K. Nakajima, T. Takahashi, *J. Am. Chem. Soc.* **1997**, *119*, 12842.
[16] M. Green, J. L. Spencer, F. G. A. Stone, C. A. Tsipis, *J. Chem. Soc. Dalton Trans.* **1977**, 1525.
[17] a) E. Block, L. K. Revelle, *J. Am. Chem. Soc.* **1978**, *100*, 1630; b) P. B. Valkovich, W. P. Weber *Tetrahedron Lett.* **1975**, *26*, 2153; c) H. Gilman, W. H. Atwell, *J. Am. Chem. Soc.* **1965**, *87*, 2678.
[18] H. Sohn, J. Merritt, D. R. Powell, R. West, *Organometallics* **1997**, *16*, 5133.
[19] L. Parkanyi, *J. Organomet. Chem.* **1981**, *216*, 9.
[20] a) V. K. Bel'skii, A. V. Dzyabchenko, *J. Struct. Chem.* **1985**, *26*, 78; *Zh. Strukt. Khim.* **1985**, *26*, 94; b) A. L. Spek, *Cambridge Crystallographic Data Centre*, CCDC-140799; c) Y. Liu, T. C. Stringfellow, D. Ballweg, I. A. Guzei, R. West, *J. Am. Chem. Soc.* **2002**, *124*, 49.
[21] a) S. Yamaguchi, T. Endo, M. Uchida, T. Izumizawa, K. Furukawa, K. Tamao, *Chem. Eur. J.* **2000**, *6*, 1683; b) U. Pernisz, N. Auner, in *Organosilicon Chemistry IV: From Molecules to Materials* (Eds.: N. Auner, J. Weis), VCH, Weinheim **2000**, p. 505.
[22] Z. Rappoport, Y. Apeloig, *The Chemistry of Organic Silicon Compounds, Vol. 3*, Wiley, New York, **2001**.
[23] D. Yan, A. A. Hess, M. Backer, N. Auner, M. D. Thomson, H. G. Roskos, W. Fann, unpublished results.
[24] H. Gilman, R. D. Gorsich, *J. Am. Chem. Soc.* **1955**, *77*, 6380.

  

[25] a) M. V. Sargent, C. J. Timmons, *J. Am. Chem. Soc.* **1963**, *85*, 2186; b) W. M. Moore, D. D. Morgan, F. R. Stermitz, *J. Am. Chem. Soc.* **1963**, *85*, 829; c) F. B. Mallory, C. S. Wood, J. T. Gordon, *J. Am. Chem. Soc.* **1964**, *86*, 3094.
[26] a) W. Herrendorf, HABITUS, Program for numerical absorption correction, Universität Giessen, Giessen (Germany), **1996**; b) G. M. Sheldrick, SHELXS-97, Program for the Solution of Crystal Structures, Universität Göttingen, Göttingen (Germany), **1997**; c) G. M. Sheldrick, SHELXL-97, Program for Crystal Structure Refinement, Universität Göttingen, Göttingen (Germany), **1997**.

Received: February 1, 2007
Published online: June 26, 2007

  